

New GEO paradigm: Re-purposing satellite components from the GEO graveyard

Nicholas H. Barbara^{a,*,1}, Stéphanie Lizy-Destrez^a, Paolo Guardabasso^a, Didier Alary^{b,2}

^a Space Advanced Concepts Laboratory (SaCLab), ISAE-SUPAERO, 10 Avenue Edouard Belin, 31400, Toulouse, France

^b Airbus Defence and Space, 31 rue des Cosmonautes, 31402, Toulouse, France

ARTICLE INFO

Keywords:

GEO
On-orbit servicing
Satellite database
Space debris
Re-purposing

ABSTRACT

The rising production rate of space debris poses an increasingly severe threat of collision to satellites in the crowded Geostationary Orbit (GEO). It also presents a unique opportunity to make use of a growing supply of in-space resources for the benefit of the satellite community. “The Recycler” is a mission proposed to source replacements for failed components in GEO satellites by extracting functioning components from non-operational spacecraft in the GEO graveyard. This paper demonstrates a method of analyzing in-space re-purposing missions such as the Recycler, using real satellite data to provide a strong platform for accurate performance estimates. An inventory of 1107 satellites in the extended GEO region is presented, and a review into past GEO satellite anomalies is conducted to show that solar arrays would be in the greatest demand for re-purposing. This inventory is used as an input to a greedy selection algorithm and trajectory simulation to show that the Recycler spacecraft could harvest components for 67 client satellites with its allotted fuel budget. This capacity directly meets the levels of customer demand estimated from the GEO satellite anomaly data, placing the Recycler as a strong contender in a future second-hand satellite-component industry. Propellant mass is found to be a greater restriction on the Recycler mission than its 15-year lifetime — a problem which could be solved by on-orbit refueling.

1. Introduction

The Geostationary Orbit (GEO) is home to one of the most profitable and expensive sectors of the satellite industry. With some GEO communications satellites costing on the order of €400 million [1], each unit is a significant investment and is expected to operate to specifications over a 10–20 year lifetime. Premature failure of a GEO satellite can lead to a lengthy and expensive replacement process, as well as significant revenue losses during operational downtime before a new satellite can be procured and launched. Rather than replacing the satellite completely, or suffering a reduced lifetime, existing resources in space could be used to repair or replace the failed components in a more sustainable and cost-effective manner. Research into this field will

allow the technology and infrastructure required for in-space re-purposing to be developed, potentially making it less expensive and more feasible than alternative solutions such as launching replacement components in the future.

It is this need that the Recycler is designed to address. The Recycler would be a commercial service available to GEO satellite owners, who would submit requests for their failed satellite components, and receive replacements harvested by the Recycler spacecraft from old, non-operational satellites in the GEO graveyard³ and surrounding areas. Components would be harvested from non-operational satellites only after a contractual agreement with the owner. The legal aspects of such an agreement are beyond the scope of this study, and are discussed in Refs. [2,3]. Preliminary designs of the Recycler predict an operational

Abbreviations: GEO, Geostationary Orbit; OOS, On-Orbit Servicing; DARPA, Defense Advanced Research Projects Agency; EGO, Extended GEO; EOL, End Of Life; NORAD, North American Aerospace Defense Command; SATCAT, Satellite Catalog; TLE, Two-Line Element; COSPAR, Committee on Space Research; RDV, Rendezvous; ECI, Earth-Centered Inertial; RAAN, Right Ascension of the Ascending Node

* Corresponding author.

E-mail addresses: nbar5346@uni.sydney.edu.au (N.H. Barbara), stephanie.lizy-destrez@isae-supaero.fr (S. Lizy-Destrez),

paolo.guardabasso@isae-supaero.fr (P. Guardabasso), didier.alary@gmail.com (D. Alary).

¹ Present address: School of Aerospace, Mechanical and Mechatronic Engineering, University of Sydney, NSW 2006, Australia.

² Present address: IAA CM, Senior researcher Chaire Sirius, Toulouse, Midi-Pyrénées, France.

³ The GEO graveyard is the region approximately ± 250 km from the GEO altitude of 35 786 km. The upper zone is definitively more used, and is the focus of this study.

<https://doi.org/10.1016/j.actaastro.2020.03.041>

Received 30 November 2019; Received in revised form 12 March 2020; Accepted 26 March 2020

Available online 07 April 2020

0094-5765/ © 2020 IAA. Published by Elsevier Ltd. All rights reserved.

lifetime of 15 years for a 2.5 t spacecraft containing approximately 500 kg of fuel, which could be propelled by three xenon-fueled RIT 2X,205 gridded ion thrusters [4].

There have been numerous investigations into On-Orbit Servicing (OOS) and the life-extension of GEO satellites [5,6]. This field is at the forefront of advanced spacecraft development, with research into the state-of-the-art technology required for OOS operations spanning several decades [3,7]. However, few attempts have been made to re-purpose existing resources in space, and in particular to use those resources to restore function to faulty satellites. Perhaps the most notable proposal is the Defense Advanced Research Projects Agency (DARPA) Phoenix program. As a proof of concept, the program aimed to harvest antennas from old GEO satellites in the graveyard, and to construct new satellite buses around these antennas on-orbit [2,8]. The Recycler is similar to the Servicer/Tender (S/T) spacecraft proposed for this program in its role of performing rendezvous with, assessing, and grappling non-cooperative target⁴ satellites, and dismantling external components with robotic appendices. If it were to install these components on client spacecraft, the Recycler would additionally interact with fully and semi-cooperative satellites. Despite it being a highly innovative proposal, the scope of the Phoenix program differs from the Recycler by focusing on building new spacecraft rather than harvesting components to repair existing satellites. It therefore cannot be used to minimize the effect of costly GEO satellite anomalies on-orbit.

This paper will focus on answering three crucial questions to the development of the Recycler and future in-space re-purposing missions: what resources are available around the GEO belt, and are they useful? what is the best strategy to access those resources for GEO satellite re-purposing? and how many spacecraft could the Recycler service or harvest components from over its lifetime, given its allotted fuel budget? To answer these questions, this study predicts which components are likely to have the greatest demand for re-purposing, and summarizes this information in an inventory of all satellites in the GEO (EGO) region. The inventory includes the necessary interfacing specifications for the selected components where available. This data is used to simulate the trajectory of the Recycler as it services targets via two different mission strategies — a “depot” method where the Recycler works in tandem with a servicer spacecraft, and a “ping-pong” method where it performs servicing duties itself. Including the servicer spacecraft in any analysis is beyond the scope of this paper. Trajectory optimization is implemented in this simulation via a greedy target selection algorithm to minimize the total fuel consumption and mission duration. By evaluating the results under each strategy, this paper gives a preliminary indication of the capacity of the Recycler to service multiple spacecraft over its lifetime with the current distribution of satellites in the EGO region, and lays the groundwork for extensive future research into the Recycler and other GEO satellite re-purposing missions.

2. Satellite resources in GEO

To give a realistic estimate of the Recycler's capacity to harvest resources and restore function to GEO satellites, an inventory of satellites and their specifications in the EGO region was developed. This involved identifying which components are likely to be in the greatest demand, and which GEO satellites are likely to have compatible components that can be re-purposed. This section investigates the primary causes of GEO satellite anomalies, and presents a preliminary iteration of a satellite inventory. This inventory is based on the most suitable components for re-purposing in GEO, and can be used to design the

Recycler mission and other in-space re-purposing missions.

2.1. Component demand

For the Recycler mission to be a profitable enterprise, it is critical that it harvest components with the greatest customer demand — that is, components with high failure rates in GEO satellites. Furthermore, these components must be sufficiently modular to allow for re-purposing on different satellite buses. These two requirements restrict the range of common GEO satellite components which could feasibly be re-purposed to: solar arrays; fuel (for both chemical and electric propulsion); and other miscellaneous parts compatible between satellites of the same bus model.

Re-purposing solar arrays must be the primary focus of the Recycler due to their relatively high failure rate in GEO. Fig. 1 summarizes the causes of GEO satellite anomalies over a 30 year period. The two pie charts contain data from two different sources [9,10], and are presented separately in Fig. 1 since each source categorizes the anomalies in a different way. After anomalies related to improper orbit insertion, specific payloads, and miscellaneous internal failures, the most common sources of malfunctions are solar arrays. Given that solar arrays are the only source of power for the majority of GEO satellites, it is crucial that they function as designed to preserve End Of Life (EOL) operational goals, and to prevent mission failure. Since solar arrays are highly modular by nature, they are also suitable candidates for re-purposing. It is therefore likely that replacing solar panels in GEO would be a market with high customer demand.

After solar arrays, issues with propulsive systems, and by extension fuel depletion, are the most common according to Fig. 1. Given that inclination drift in GEO is on the order of 0. 9° per year [11], a satellite with a failed propulsive system could drift significantly from its allotted GEO slot before meeting EOL goals. However, removing and replacing thrusters on-orbit is not currently a realistic goal for the Recycler. The complexities of such an operation are too great, and would require a highly modular design of thrusters, fuel-feed systems, and power processing units (for electric propulsion) to ensure a minimum level of compatibility between satellites. A more achievable task is refueling, which could be attempted to meet the demand of failure due to fuel depletion, or indeed as a life-extension strategy. It can be assumed that on-orbit refueling will be a developed technique by the time the Recycler is designed and launched, given the numerous current and previous proof-of-concept missions, such as DARPA's Orbital Express mission [12], National Aeronautics and Space Administration's Restore-L mission [13], and Airbus Defence and Space's O.CUBED services [14].

Other components, such as radiators and louvers or structural components, could potentially be interchanged between satellites of the same bus design given the appropriate tools. However, they are unlikely to be compatible between satellites of different buses due to the specific geometries of such components to each satellite, and would not be in high demand according to Fig. 1. “Other parts” such as these are accounted for in the satellite inventory for rare anomalies, but should not be the focus of the Recycler mission. Additional important components such as antennas, attitude control systems, and payloads are either located too internally in most GEO satellites to be feasibly extracted on-orbit, or are too mission-specific to be transferred to a new spacecraft. More modular spacecraft designs, and improved compatibility between bus models, are critical for these vital components to ever be re-purposed. While this presents an interesting challenge for the future, such components are not currently good candidates for re-purposing, and are beyond the scope of this paper.

2.2. The EGO satellite inventory

The EGO satellite inventory is a repository of all operational and non-operational satellites in the EGO region, and their interfacing specifications relevant to solar arrays, propellants, and bus models,

⁴ It is convention in the space rendezvous community to use the term “target” for a visited satellite. A target may also be thought of as a “donor” satellite in the context of the Recycler, as it is a potential source of replacement components.

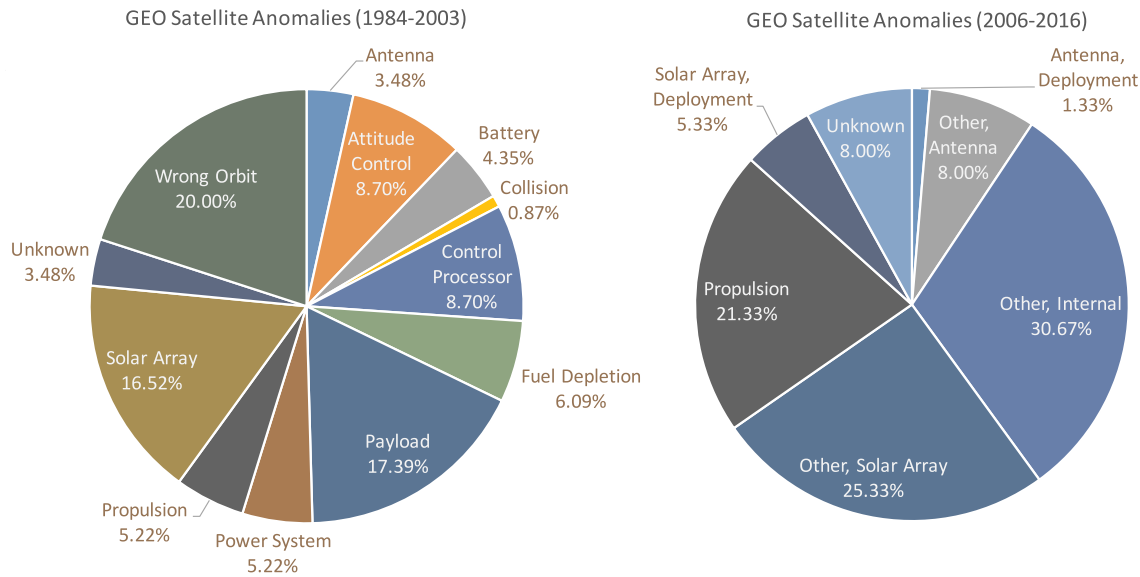


Fig. 1. Summary of GEO satellite anomalies and mission failures from 1984 to 2016. The charts on the left and right were compiled using data published in Ref. [9,10], and account for 115 and 75 anomalies, respectively.

Table 1

Extract from the EGO satellite inventory, showing data for 3 of the 1107 satellites. Fields from the Committee on Space Research (COSPAR) ID to the Inclination are based on the NORAD SATCAT, and are described in detail in the documentation [15].

Field	Satellite 1	Satellite 2	Satellite 3
COSPAR ID	1997-009A	2005-036A	2012-035A
NORAD ID	24742	28868	38551
Operational Status	*_	*+	*+
Name	INTELSAT 801 (IS-801)	ANIK F1R	ECHOSTAR 17
Owner	ITSO	CA	US
Launch Date	1997-03-01	2005-09-08	2012-07-05
Launch Site	FRGUI	TYMSC	FRGUI
Mean Motion (revs/day)	0.987316	1.002716	1.002716
Semi-Major Axis (km)	42601.137	42164.637	42165.137
Eccentricity	0.0014319	0.0002016	0.0002134
Inclination (°)	7.8	0.0	0.0
Bus Model	AS-7000	Eurostar-3000S	SSL-1300
Bus Voltage (V)	100	50	100
Max Power (kW)	4.8	10.0	16.1
Fuel (Chemical)	MON/Hydrazine	MON/MMH	MON/MMH
Fuel (Electric)	–	–	Xe

provided that the information is publicly available. An extract is provided in Table 1. Based on the North American Aerospace Defense Command (NORAD) Satellite Catalog (SATCAT) [15], it contains information on the identification number, name, status, ownership, and basic orbital parameters for the 1107 tracked satellites in the EGO region (as of January 21, 2019). This region is defined by the European Space and Operations Centre (ESOC) as the range of geocentric orbits with semi-major axis $37\,948 < a < 46\,380$ km, eccentricity $e < 0.25$, and inclination $0^\circ < i < 25^\circ$ [16]. Two-Line Element (TLE) data is included alongside the inventory for the 584 satellites with available data, and was extracted from the NORAD Master TLE Index [17]. This makes it possible to reconstruct the orbits of more than half of the satellites in the inventory, giving accurate data to estimate the fuel and time costs required for the Recycler to reach each satellite (Sec. 3). Orbiting bodies other than spacecraft in the EGO region, such as debris, rocket bodies, or detached apogee kick motors, are not included in the inventory.

In addition to the information extracted from the SATCAT and the

TLE data, the EGO inventory contains the five custom fields shown in Table 1. These relate to the interfacing requirements of GEO satellite components, and must be appropriately matched for a component to be considered transferable between satellites. The first is the satellite bus model. This is a general indicator of compatibility with the other satellites in the inventory, where it is assumed that some miscellaneous components are transferable between satellites of the same bus architecture. Satellite bus information was primarily obtained from Ref. [18]. Second to this is the satellite bus voltage. This is typically dependent on the satellite bus, and must be matched to re-purpose electronic components — in particular, the solar arrays. Much of the bus voltage information came from Ref. [19,20].

Likewise, the maximum power delivered by solar arrays is crucial information when sourcing a replacement array. That is, the replacement array must be capable of supplying greater than or equal to the maximum power required by the client satellite. EOL estimates were always used where available. However, a lack of public information on many satellites means that Beginning Of Life (BOL) estimates were quoted for maximum power in some cases. The majority of maximum power information was sourced from the Union of Concerned Scientists’ satellite database [21]. Fuel used for both chemical and electric thrusters is also recorded in the final two fields of the inventory, where applicable. The most common chemical fuel was a MON/MMH mixture used in bipropellant thrusters. Xenon is the only “electric” propellant in the inventory, as it is currently the dominant available technology. Fuel information for each satellite was sourced from a combination of [22,23].

Fig. 2 demonstrates how the inventory can be used to gain insight into aspects of re-purposing missions, showing the distribution of bus models and bus voltages in the EGO region as an example. As expected, more recent buses (Eurostar-3000, BSS-702) have fewer non-operational counterparts from which components could be harvested, whereas some older models (BSS-601) have almost twice as many. The same is true for bus voltages, where there are very few non-operational satellites at the higher voltages (70 V, 100 V) used on modern satellite buses. The 50 V bus voltage column sees the most overlap between operational and non-operational satellites in Fig. 2, as it is used for both older (BSS-601, BSS-601HP) and more recent bus models (Eurostar-3000). Satellites operating in this voltage range therefore appear to be the best candidates for re-purposing in the current EGO satellite climate. By the time the Recycler is launched, there are likely to be many

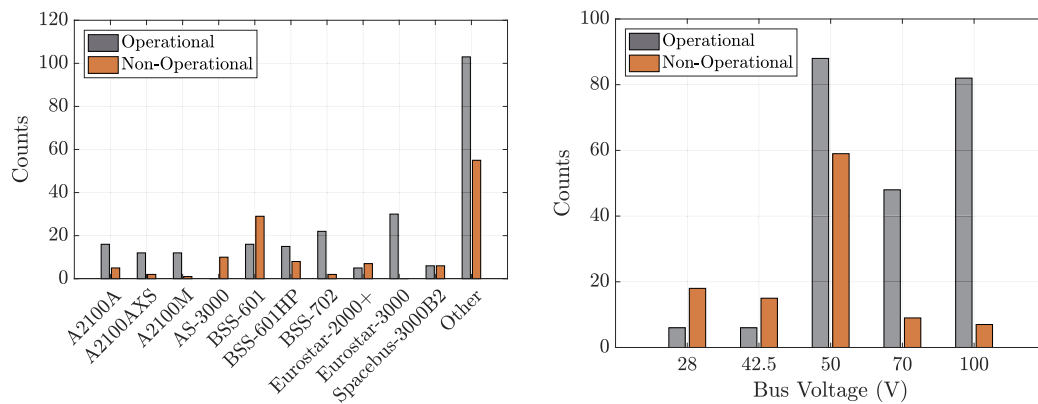


Fig. 2. Distribution of bus models (left) and bus voltages (right) in the EGO inventory. A total of 362 and 338 satellites have bus model and bus voltage information currently in the inventory (respectively). Bus types with fewer than 10 counts are collected in the “Other” category for the purposes of this figure.

more non-operational satellites in the EGO region that have been designed from some of today's more recent bus models, with higher bus voltages. A move to more modular spacecraft bus designs, with compatible systems across multiple models, would see a growth in the supply of non-operational satellites with the required specifications for re-purposing in the future.

It must be noted that while the satellite inventory is a useful tool for summarizing the resources available in the EGO region, it is by no means exhaustive. Many satellites do not have the required interfacing information filled in for each field, either due to the lack of publicly available information, or the extensive manual labor required to complete the inventory. Furthermore, the basic orbital elements in the inventory (Table 1) obtained from the SATCAT do not include important information such as the argument of perigee or true anomaly of each satellite in its orbit, meaning orbits can only be reconstructed for the satellites with available TLE data. The majority of the 584 satellites with TLE data in the inventory are operational satellites, and hence there is a lack of orbital information on the non-operational satellites from which the Recycler would harvest components. Therefore, the results discussed in Section 3, in which the EGO satellite inventory is used as a mission analysis tool, are only preliminary estimates of the operational capability of the Recycler. The effects of this limitation are discussed further in Sections 3.2 and 3.3.

3. Recycler mission analysis

With the EGO satellite inventory summarizing the available resources in and around the GEO belt for component re-purposing, its usefulness as a mission analysis tool can now be demonstrated. In this section, two potential mission strategies for the Recycler are outlined, and the spacecraft trajectory is simulated to estimate the fuel and time costs of harvesting satellite components in each case. This is concluded by evaluating the performance of the Recycler under each strategy, estimating how many spacecraft the Recycler could service in its lifetime given its allotted fuel budget.

3.1. Mission strategies

A high-level overview of the Recycler's operations sequence is shown in Fig. 3. A list of client requirements will be submitted to the Recycler contractor outlining the needed components, and the Recycler ground team will run an optimization program to select a list of targets from the EGO satellite inventory with matching components for each client. The Recycler will approach each target on this list in the specified order to minimize fuel consumption and time taken, and assess its current state. The ground team must decide whether or not to engage with the target according to the conditions it is observed to be in. If the decision is a “NOGO,” a new target must be selected. In the case of a

“GO” decision, the Recycler will complete its approach to grapple the target, berth with it, and commence disassembly operations on the required components.

The two methods considered in this paper for depositing components harvested from the target spacecraft are a “depot” method and a “ping-pong” method. A visual overview of each strategy is presented in Fig. 4. Both rely on a “Space Factory” — a large spacecraft with several ports in which satellite components could be stored for extended time periods. The Space Factory would have robotic arms for interacting with other spacecraft and for performing its own operations, and could potentially have the capacity to refuel spacecraft while they are docked. It is assumed that the Space Factory would be in orbit 100 km above the GEO belt. It would therefore be near the Recycler's zone of operation, but would not occupy high-demand GEO slots nor interfere with transmitted signals from GEO satellites, and would be sufficiently far from the GEO graveyard to avoid a high probability of collision with debris. In the depot strategy, the Recycler delivers the harvested satellite components from a target to the Space Factory, which acts as a central “depot”. Conversely, in the ping-pong strategy, the Recycler must deliver and install the harvested components directly to the client satellite itself, before returning the failed components from the client to the Space Factory to avoid generating debris. After completing either procedure, the Recycler will repeat with a new target and client until it services its final target, its lifetime expires, or it exceeds its propellant budget.

The key difference between the two methods in Fig. 4 is the need for a servicer spacecraft, such as the S/T proposed for the Phoenix program (Sec. 1). In the depot method, a servicer is required to retrieve the harvested components from the Space Factory and to install them on a client satellite. A servicer is depicted working alongside the Recycler and the Space Factory in Fig. 4a. The advantage of this method is that the Recycler does not interact with the client satellite, only delivering the required components to a central location from which servicing missions can be launched. This would allow the two spacecraft to operate in parallel, potentially making the mission more time-efficient. It could also facilitate the repair of minor damages to components (such as solar arrays) due to micrometeoroids, radiation, and other effects of the space environment while on-board the Space Factory.

The ping-pong method is an extension of the Recycler's responsibilities from the depot method, and assigns the role of servicing client satellites to the Recycler itself. Although this eliminates the need for a servicer spacecraft, the Recycler must therefore perform an extra set of operations on the client satellite before returning to the Space Factory, as per Fig. 4b. While this is significantly more time consuming than the depot approach, relying on fewer spacecraft may require a smaller initial budget for a proof-of-concept Recycler mission. The ping-pong method is therefore to be considered separately from the depot method, and only for missions where the Recycler cannot operate alongside a servicer spacecraft.

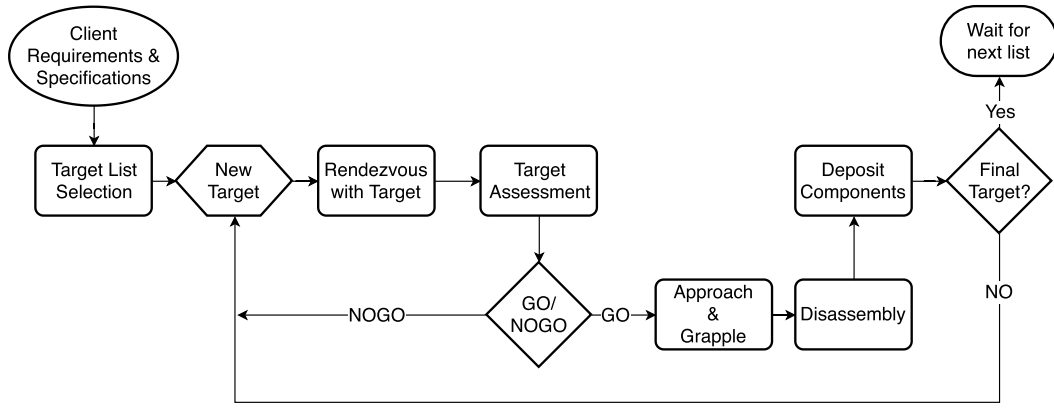


Fig. 3. High-level overview of the proposed spacecraft operations sequence for the Recycler.

3.2. Trajectory simulation

To investigate the performance of the Recycler under these two strategies, a MATLAB simulation was developed to model its trajectory over a typical 15-year mission lifetime. The simulation builds an ordered list of targets from which to harvest components for a given list of client satellites. Targets are ordered according to a greedy selection algorithm, with the lowest-cost target first on the list [24]. An overview of the algorithm is provided in Fig. 5. Customer requirements, consisting of a desired component (such as a solar array) for each client satellite, are checked against the EGO satellite inventory. All satellites in the inventory with matching specifications (Sec. 2.2), and within a given range of Keplerian orbital elements, are supplied to the greedy selection algorithm as potential targets.

For each client satellite, the simulation computes the trajectory of the Recycler from its current state to every remaining candidate target, and selects the target “costing” the least to reach. This cost is evaluated according to two criteria: a fuel cost, characterized by the increase in velocity, ΔV , supplied by the propulsion system; and the total time taken, Δt . The satellite with the lowest cost is added to the next slot in the target list, and the process is repeated provided the Recycler has sufficient fuel to complete the maneuver, and has not exhausted its lifetime. Target satellites meeting requirements for multiple clients are assigned to the customer highest up on the client list, operating on a “first-in-first-served” basis. More complex situations, such as simultaneous client requests, incorporating a client priority scheme, or accounting for the relative necessity of components for one client satellite over another, are to be addressed in future studies of the Recycler. The same is true for additional cost criteria, such as the age and functionality of target satellites and their components (Sec. 4).

As discussed in Section 2.2, more non-operational satellites with complete information in the EGO inventory are required for only these spacecraft to be considered as potential targets in the model. For this reason, the simulation also considers any operational satellites in the inventory that are not client satellites as potential targets. It is strongly recommended that the same methods presented in this paper be applied with a complete inventory, and only non-operational satellites as targets, for an improved estimate of the Recycler’s performance in the next phases of the mission design process.

3.2.1. Transfer-orbit model

To assign ΔV and Δt costs to each individual target at each iteration of the greedy algorithm, the Recycler was simulated performing transfers between its initial position, each target, and the Space Factory in the depot method, and between its initial position, each target, the respective client, and the Space Factory in the ping-pong method (Fig. 4). Each trajectory was modeled as an open-loop, low-thrust transfer in the unperturbed two-body problem between two circular

orbits. The equations of motion describing the spacecraft position \mathbf{r} and velocity \mathbf{v} in the Earth-Centered Inertial (ECI) coordinate frame, in addition to the total mass m , as functions of time are

$$\dot{\mathbf{r}} = \mathbf{v} \quad (1)$$

$$\dot{\mathbf{v}} = -\frac{\mu}{\|\mathbf{r}\|^3} \mathbf{r} + \mathbf{\Gamma} \quad (2)$$

$$\dot{m} = -\frac{T}{g_0 \cdot \text{Isp}} \quad (3)$$

Here, $\mu = 3.9860 \times 10^{14} \text{ m}^3/\text{s}^2$ is the gravitational parameter for Earth [25], $\mathbf{\Gamma}$ is the thrust acceleration vector in the ECI frame, and T is the total thrust. The rate of fuel consumption \dot{m} depends on the engine specific impulse, Isp , and the standard gravitational acceleration on Earth’s surface, $g_0 = 9.80665 \text{ m/s}^2$. A constant thrust and Isp of 594 mN and 2450 s were assumed (respectively). These values correspond to a propulsion system consisting of three RIT 2X_205 gridded ion thrusters [4] chosen in a previous system-level preliminary design. It is strongly recommended that a detailed investigation into the sensitivity of the Recycler’s performance to these two parameters be conducted, as it may provide useful insight into the peak mission performance. Such a study is beyond the scope of this paper, and has been left for future investigations of the Recycler (Sec. 4).

The thrust acceleration vector $\mathbf{\Gamma}$ was computed using the Edelbaum optimal thrust profile for transfers between two non-coplanar circular orbits [26,27]. In terms of radial, normal, and tangential components to the spacecraft orbit,

$$\mathbf{\Gamma} = 0 \mathbf{i}_r + \frac{T}{m} \sin(\beta) \mathbf{i}_n + s \frac{T}{m} \cos(\beta) \mathbf{i}_t \quad (4)$$

with

$$\mathbf{i}_r = \frac{\mathbf{r}}{\|\mathbf{r}\|}, \quad \mathbf{i}_n = \frac{\mathbf{r} \times \mathbf{v}}{\|\mathbf{r} \times \mathbf{v}\|}, \quad \mathbf{i}_t = \mathbf{i}_n \times \mathbf{i}_r, \quad (5)$$

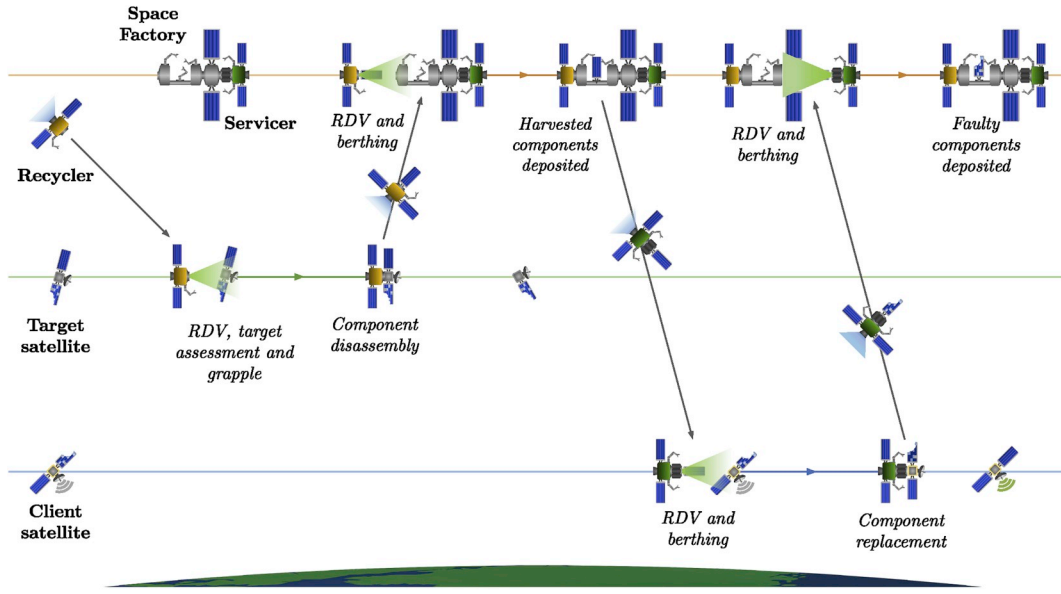
where $s = +1$ if the transfer must increase the orbital altitude, and $s = -1$ for a decrease in altitude. The out-of-plane yaw angle, β , is governed by

$$\beta(t) = \tan^{-1} \left(\frac{v_0 \sin(\beta_0)}{v_0 \cos(\beta_0) - \frac{T}{m} t} \right), \quad (6)$$

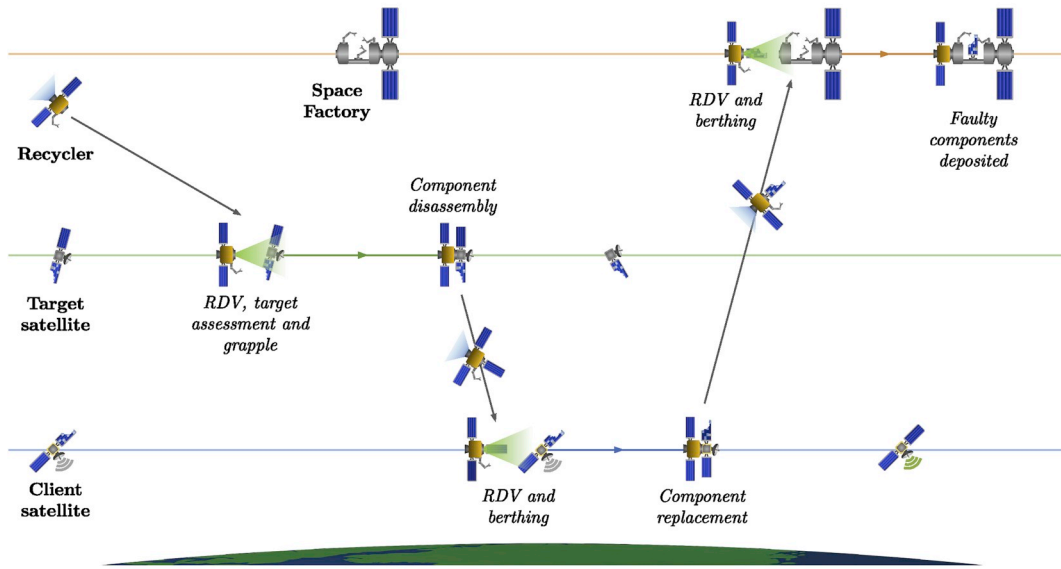
where

$$\beta_0 = \tan^{-1} \left(\frac{\sin\left(\frac{\pi}{2} \Delta i\right)}{\frac{v_0}{v_f} - \cos\left(\frac{\pi}{2} \Delta i\right)} \right). \quad (7)$$

In Equations (6) and (7), v_0 is the initial orbital velocity of the spacecraft, and v_f is the desired final orbital velocity. Δi is the total



(a) Depot strategy.



(b) Ping-pong strategy.

Fig. 4. Visual overview of the Rendezvous (RDV) and operations strategies for the Recycler, and its interactions with the Space Factory and a servicer spacecraft. Note that no servicer is required for the ping-pong strategy.

angular change required for the maneuver, including both a change in inclination i and in Right Ascension of the Ascending Node (RAAN), Ω . For initial RAAN and inclination Ω_1, i_1 , and final RAAN and inclination Ω_2, i_2 , this angular change is

$$\cos(\Delta i) = \sin i_1 \sin i_2 \cos(\Omega_1 - \Omega_2) + \cos i_1 \cos i_2. \quad (8)$$

If the initial and final orbits are exactly coplanar, then $\Delta i = 0$ and $\beta = 0$ for all t . It should be noted that $\beta(t)$ is piecewise constant, with the sign changed at the orbital anti-nodes to ensure a plane change can occur [27].

These equations of motion were integrated numerically in MATLAB using a Runge-Kutta fourth-order scheme. The phasing time Δt_{phase} that the Recycler must wait in its initial orbit before starting a transfer to meet its target directly at the correct true anomaly was also computed. Suppose the Recycler initiated a transfer immediately at the start of

each rendezvous computation. The angle by which the target and Recycler would be out of phase in the target orbit is $\Delta\varphi = L_t - L_2$, where L_t and L_2 are the true longitudes of the target and Recycler at the end of the transfer, respectively. If the Recycler begins with an initial orbital rate ω_1 and ends at the target orbital rate of ω_t , the “time to wait” in the initial orbit to match the final phase between the two spacecraft is

$$\Delta t_{\text{phase}} = \frac{\Delta\varphi}{\omega_1 - \omega_t}. \quad (9)$$

In this simplified model, the Recycler decreases its altitude by 500 km if the predicted phasing time is greater than a month, since a greater difference in orbital rates between the initial and final orbits greatly reduces the phasing time by Equation (9), albeit for a small ΔV cost. It should be noted that while the Edelbaum profile assumes the

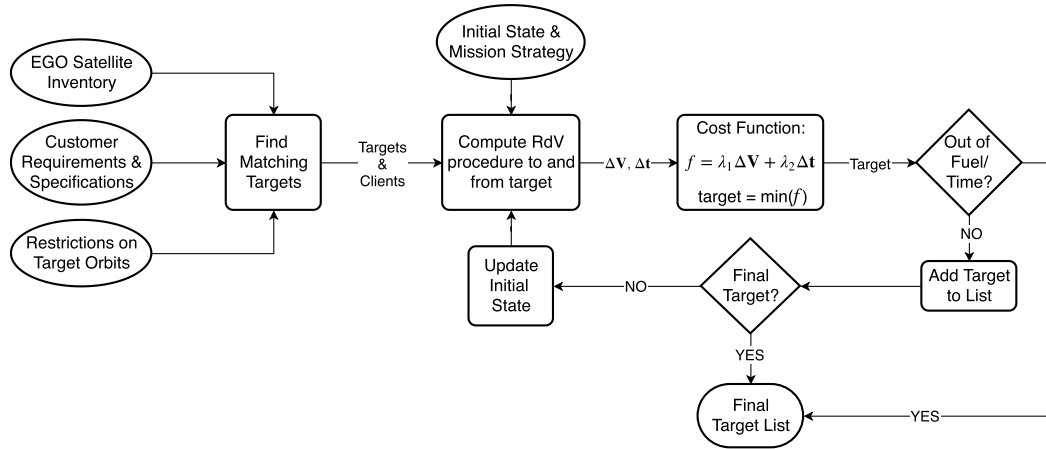


Fig. 5. Flow chart depicting the greedy target selection architecture.

spacecraft supplies an infinitesimal thrust at constant thrust acceleration, and will therefore not exactly meet the target orbit in each transfer, the effect has negligible impact on the estimated ΔV and Δt . The same is true for closed-loop approach maneuvers and station-keeping about a target during the assessment phase, which have been neglected. The assumption of circular orbits in this analysis is also a good approximation, as 98.5% of satellites in the EGO region have eccentricity $e < 0.01$ [15].

3.2.2. Cost estimation

To choose an optimum target from which to harvest components at each iteration of the greedy algorithm in Fig. 5, the cost of interacting with a target (depot) or target-client pair (ping-pong) must be evaluated. Let ΔV_k and Δt_k be the total ΔV and Δt costs for the k^{th} target at a single iteration of the algorithm. Summing over all transfers $j = 1, \dots, j_{\max}$ performed by the Recycler in each mission strategy gives

$$\Delta V_k = \sum_{j=1}^{j_{\max}} \Delta V_j, \quad \Delta t_k = \Delta t_{\text{ops}} + \sum_{j=1}^{j_{\max}} \Delta t_j. \quad (10)$$

The Recycler performs a total of $j_{\max} = 2$ and $j_{\max} = 3$ transfers under the depot and ping-pong strategies (respectively), as per Fig. 4. The quantity Δt_{ops} in Equation (10) represents the estimated time for operations performed under each mission strategy, and is constant across all targets k . In their work on the Phoenix program, DARPA recommend that approximately 1 week be allowed for proximity operations about a target, 1–2 weeks for inspection, and 1 week for target anomaly resolution [28]. Adding 1 week to extract components after docking with a target, and 1 week to interact with the Space Factory, gives a conservative estimate of $\Delta t_{\text{ops}} = 6$ weeks per target for the depot method. For the ping-pong method, an additional 3 weeks were included for interacting with and upgrading the client satellite, giving $\Delta t_{\text{ops}} = 9$ weeks per target.

The final cost associated with every target at each iteration of the greedy selection process in Fig. 5 can be expressed in terms of a cost function. Suppose that there are N remaining candidate targets which have not yet been selected in previous iterations of the algorithm, and let $\Delta \mathbf{V} = (\Delta V_1, \dots, \Delta V_N)$, $\Delta \mathbf{t} = (\Delta t_1, \dots, \Delta t_N)$, with $k \in [1, N]$. The cost \mathbf{f} is defined by the weighted sum of the fuel and time costs,

$$\mathbf{f} = \lambda_1 \Delta \mathbf{V} + \lambda_2 \Delta \mathbf{t}, \quad (11)$$

for scalar weighting coefficients $\lambda_1, \lambda_2 \in [0, 1]$ such that $\lambda_1 + \lambda_2 = 1$. Given that $\Delta \mathbf{V}$ and $\Delta \mathbf{t}$ represent physically different quantities, each vector must be normalized prior to the summation in Equation (11). This was ensured with a scaled robust sigmoid [29], as described by Equation (12). A vector \mathbf{x} of arbitrary values is converted to a normalized vector \mathbf{y} , with each element $y_k \in [0, 1]$, via an intermediate

variable $\hat{\mathbf{y}}$:

$$\mathbf{y} = \frac{\hat{\mathbf{y}} - \min(\hat{\mathbf{y}})}{\max(\hat{\mathbf{y}}) - \min(\hat{\mathbf{y}})} \quad \text{where} \quad \hat{\mathbf{y}} = \frac{1}{1 + e^{-\frac{\mathbf{x} - m}{r/1.35}}}. \quad (12)$$

Here, m and r are the median and interquartile range of \mathbf{x} , respectively. This method is particularly robust against outliers skewing the normalization, allowing for a fair comparison of all targets. Since $\Delta V_k, \Delta t_k \geq 0$ for all targets k by definition of the quantities, the “optimum” target k for the Recycler to next approach from its current orbital state must therefore minimize the cost function, such that $f_k = \min(\mathbf{f})$. It is this k^{th} satellite that is added to the target list in Fig. 5.

Equal cost weightings of $\lambda_1 = \lambda_2 = 0.5$ were used in this study to give a preliminary indication of the mission performance. In the worst case, this weighting combination is the best possible, giving an upper limit on the performance of the Recycler. This assumes that the consumption of fuel in harvesting components from a given target, and the time taken to do so, are of equal importance to the optimal operation of the Recycler. In reality, it is likely that fast delivery of components to a GEO client satellite would be preferred to minimize costly down-time. This would certainly be the case if, for example, the Recycler had the opportunity to re-fuel at the Space Factory. Even if this were the case, ΔV would remain in the cost function, albeit with a lower weighting, to minimize the Recycler’s fuel consumption and reduce the total mission expenditure. Much like the thrust and Isp discussed in Section 3.2.1, future studies of the Recycler should include a detailed sensitivity analysis of these cost function weightings to determine their impact on the predicted mission performance (Sec. 4).

3.3. Performance evaluation

The trajectory simulation outlined in Section 3.2 was applied both to the depot and ping-pong missions strategies to estimate the maximum performance capacity of the Recycler over its mission life in each case. The results are presented in Fig. 6. A total of 89 operational client satellites were randomly selected from the EGO inventory, with random components assigned to each out of solar arrays, chemical and electric fuel re-supply, and “other parts” (Sec. 2). The remaining 123 satellites in the inventory with available information were assigned as potential targets from which to choose. No restrictions were placed on the orbits of the target satellites, other than the criteria that they be in the EGO region. Of the 89 clients, the Recycler could harvest components for 67 when using the depot method, and service 27 clients using the ping-pong method, before consuming its allotted fuel budget. It should be noted that the results in Fig. 6 for the depot strategy do not include the ΔV costs of the servicer spacecraft (Fig. 4a). Accounting for this additional fuel would increase the total mission cost, but would not limit the

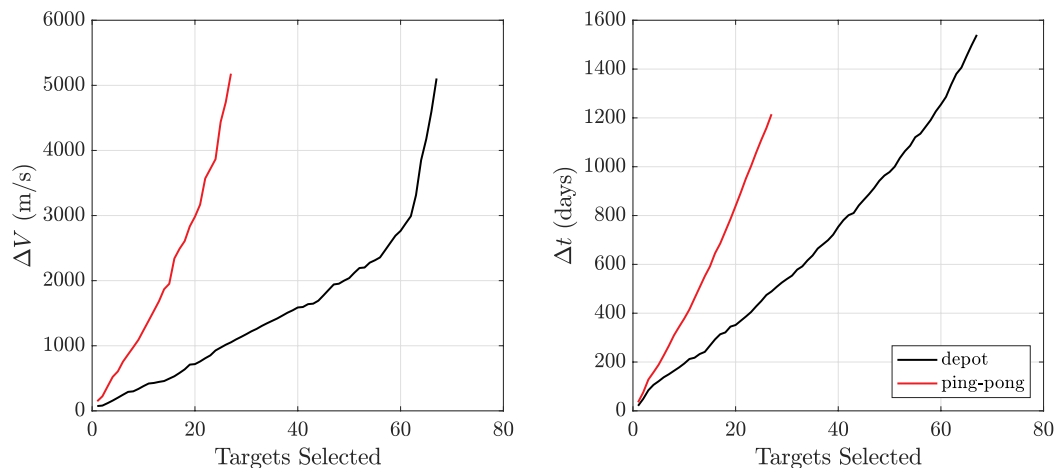


Fig. 6. Comparison of cost for the two mission strategies examined, where targets selected denotes the number of targets chosen at each iteration of the greedy algorithm. Note the sharp increase in ΔV in the depot method after servicing approximately 60 targets.

number of client satellites serviced in a given time period.

It is interesting to note that propellant supply was the limiting factor for the Recycler rather than its lifetime under the chosen simulation conditions. This is likely to be the case for all reasonable choices of thrust, Isp, and cost function weightings given that the Recycler expended its fuel budget only 4 years into its 15-year lifetime in Fig. 6. If it is assumed that the Space Factory has the resources to refuel the Recycler during the regular interaction between the two spacecraft, propellant supply would no longer be a restriction. In this case, the Recycler could harvest components for over 200 clients under the depot strategy, or service over 100 clients under the ping-pong method, as determined by linearly extrapolating the number of targets visited up to 15 years. Given that Fig. 1 suggests that there are approximately 6–7 GEO satellite anomalies recorded on average each year, the Recycler would therefore be able to meet customer demand in a second-hand satellite-components market when using either method.

The trend of an increasing ΔV slope as more targets are added in Fig. 6 is both an artifact of the greedy algorithm outlined in Section 3.2.2, and an interesting result regarding the effect of target inclination. The algorithm preferences the selection of low-cost targets at each iteration. Given that performing a large plane-change maneuver costs far more ΔV and time than only changing altitude, and that the Recycler began the simulation at the Space Factory in a GEO +100 km orbit at $i = 0^\circ$ inclination, the algorithm favored targets in the equatorial plane. Furthermore, since the possible targets were not restricted to non-operational targets due to the incomplete EGO inventory, the large number of operational satellites exactly in Geostationary Orbit were available for selection. This explains the almost uniform increase in ΔV in the depot method in Fig. 6, until approximately 60 targets were selected. It was at this point that the algorithm no longer had potential targets at $i \approx 0^\circ$ to select, and forced the Recycler into higher-inclination orbits and larger plane changes.

If potential targets were limited to only non-operational, non-military satellites in the EGO region, the distributions in Fig. 7 suggest that the Recycler would have to operate at inclinations $i \gg 0^\circ$ to approach useful targets. It therefore may appear as if the results in Fig. 6 are overestimating the performance of the Recycler under more realistic conditions, where larger and more frequent plane changes could be required. However, the time taken to service each target in Fig. 6 does not dramatically increase when performing rendezvous at higher inclinations as the ΔV curve does — indeed, it is approximately linear as more targets are selected. This reinforces the fact that the increased strain on the propellant budget is the primary concern, and that with the ability to refuel, the number of targets serviced by the Recycler estimated in this study is a good first approximation of its potential

capability. Furthermore, if the Recycler were to shift its zone of operation to higher inclinations, only harvesting components from the many non-operational satellites at, for example, a restricted range of $12^\circ < i < 15^\circ$ (Fig. 7), regular and significant plane changes would not be required. Provided the Space Factory was relocated to this same region, the steep rise in ΔV as more targets are added would not be observed. The capacity of the Recycler predicted in this paper is therefore a good first estimate of its mission capacity under more realistic scenarios.

4. Conclusions

This paper has presented a method of analyzing in-space re-purposing missions that is founded on real satellite data, showing that it provides a strong platform for realistic and valid performance estimates. An inventory of the satellite resources available in the EGO region was compiled, showing that the focus of GEO satellite re-purposing must be on solar arrays. This inventory was used alongside a greedy selection algorithm and trajectory simulation to investigate two mission strategies for the Recycler (depot and ping-pong), finding that the spacecraft could harvest components from 67 targets when working with a servicer, and could supply components to 27 clients when tasked with servicing duties itself. In doing so, this paper has shown that the propellant budget is the primary restriction on the lasting operation of the Recycler, and that with refueling capabilities, the Recycler can meet the expected market demand for the duration of its 15-year lifetime.

This paper has laid the groundwork for substantial further research into the Recycler concept and other in-space re-purposing missions. Future work on the Recycler mission must continue to be based on satellite inventories, and the EGO inventory presented in this paper must be further expanded upon to include information on more non-operational satellites. Additional data will allow for more robust analysis methods of the Recycler mission, such as a Monte Carlo simulation to average out the sensitivity of the results to the chosen candidate targets, clients, and their respective inclination distributions. This data will also be critical in analyzing more complex and realistic mission scenarios. Examples include investigating the effect of the spacecraft encountering a “NOGO” result during target assessment (Fig. 3), and determining a client-satellite hierarchy based on the relative need for components and their availability.

These scenarios must also be combined with a refined version of the trajectory simulation outlined in this paper. It is strongly recommended that a more complex target-phasing strategy be implemented, and that a more sophisticated optimization scheme be used with additional elements integrated into the cost function. Potential additions to the

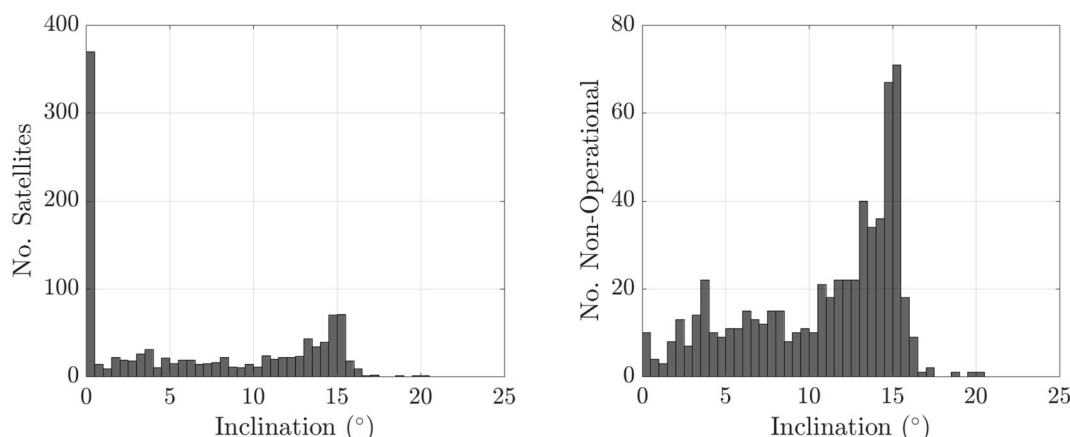


Fig. 7. Distribution of all satellites (1107), and only non-operational satellites (617), contained in the EGO satellite inventory as a function of inclination.

cost function include a client priority metric, and the age of target satellite components — a particularly important consideration for solar arrays, which degrade even when not in use due to the space environment. The optimal thrust, Isp, and weightings of the cost-function coefficients must also be investigated via a sensitivity analysis, both with and without the assumption that the Recycler may refuel at the Space Factory. Additionally, substantial research into the legal, technical, and financial aspects of gaining authorization from the owner of a potential target satellite to harvest components must be conducted. These crucial additions will further strengthen estimates of the capacity of the Recycler to harvest GEO satellite components, and give broader insight into the feasibility of future in-space re-purposing missions.

Declaration of competing interest

None.

Acknowledgments

The authors gratefully acknowledge the ISAE-SUPAERO team who worked on the initial proposal for the Recycler project: Rozenn Robidel, Olivier Finiel, Justine Guilleumou, Pol Vidal Martinez. Special thanks are extended to Laurent Beauregard and Emmanuel Blazquez for many helpful discussions during this research. This work was funded by SaCLab (grant number 2017-CIF-R-18), a research group of ISAE-SUPAERO, and by the Nicolas Baudin Internships in France Initiative for 2018/19 (internship contract number 2018-CIF-D-55).

References

- [1] W. Mott, R. Sheldon, *Laser Satellite Communication: the Third Generation* vol. 88, Quorum Books, 2000 Post Road West, Westport, CT 06881.
- [2] D. Barnhart, B. Sullivan, R. Hunter, J. Bruhn, E. Fowler, L.M. Hoag, S. Chappie, G. Henshaw, B.E. Kelm, T. Kennedy, M. Mook, K. Vincent, Phoenix Program Status — 2013, AIAA SPACE 2013 Conference and Exposition, 2013, <https://doi.org/10.2514/6.2013-5341>.
- [3] Goddard Space Flight Center, On-orbit Satellite Servicing Study Project Report, Tech. Rep. NP-2010-08-162-GSFC, National Aeronautics and Space Administration, Greenbelt, MD, 2017 Oct. 2010 https://spsd.gsfc.nasa.gov/servicing_study.html.
- [4] ArianeGroup, Electric propulsion systems and components, Ariane group orbital propulsion Centre, [Accessed February 14, 2019]. URL <http://www.space-propulsion.com/brochures/electric-propulsion/electric-propulsion-thrusters.pdf>.
- [5] J.P. Davis, J.P. Mayberry, J.P. Penn, On-orbit Servicing: Inspection, Repair, Refuel, Upgrade, and Assembly of Satellites in Space, The Aerospace Corporation Center for Space Policy and Strategy, Apr. 2019.
- [6] J.N. Pelton, On-Orbit Servicing and Retrofitting, Springer International Publishing, Cham, 2017, pp. 1237–1255, https://doi.org/10.1007/978-3-319-23386-4_104.
- [7] D.L. Akin, M.L. Minsky, E.D. Thiel, C.R. Kurtzman, Space Applications of Automation, Robotics and Machine Intelligence Systems (Aramis), Phase 2. Volume 1: Telepresence Technology Base Development, Tech. Rep. NASA-CR-3734, National Aeronautics and Space Administration, Massachusetts Inst. of Tech. Space Systems Lab., Cambridge, MA, United States, Oct. 1983 <https://ntrs.nasa.gov/search.jsp?R=19840002515>.
- [8] B.R. Sullivan, D. Barnhart, L. Hill, P. Oppenheimer, B.L. Benedict, G. Van Ommering, L. Chappell, J. Ratti, P. Will, Darpa phoenix payload orbital delivery system (pods): fedex to geo, AIAA SPACE 2013 Conference and Exposition, 2013, <https://doi.org/10.2514/6.2013-5484>.
- [9] B.R. Sullivan, Technical and Economic Feasibility of Telerobotic On-Orbit Satellite Servicing, Ph.D. thesis, Department of Aerospace Engineering, University of Maryland, College Park, Md, Aug. 2005 <http://hdl.handle.net/1903/2330>.
- [10] G. Roesler, Program overview, robotic servicing of geosynchronous satellites (RSGS) proposers day, [Accessed January 8, 2019] (2016). URL <https://www.darpa.mil/attachments/RSGSProposersDaySlideDeck.PDF>.
- [11] J.R. Wertz, D.F. Everett, J.J. Puschell, Space Mission Engineering : the New SMAD, first ed., Microcosm Press, Hawthorne, CA, 2011.
- [12] A. Ogilvie, J. Allport, M. Hannah, J. Lymer, Autonomous satellite servicing using the orbital express demonstration manipulator system, Proceedings of the 9th International Symposium on Artificial Intelligence, Robotics and Automation in Space, iSAIRAS, 2008.
- [13] B. B. Reed, R. C. Smith, B. J. Naasz, J. F. Pellegrino, C. E. Bacon, The restore-1 servicing mission, AIAA Space Conf. doi:10.2514/6.2016-5478.
- [14] O. Airbus, Cubed Services, (2019) Accessed August 10, 2019 <https://www.airbus.com/space/Services/on-orbit-services.html>.
- [15] T.S. Kelso, Satellite catalogue (SATCAT), NORAD CelesTrak, Accessed January 14, 2019] (Jul. 2019). URL <https://www.celestrak.com/satcat/search.php>.
- [16] ESA Space Debris Office, Classification of Geosynchronous Objects, Tech. Rep. GEN-DB-LOG-00211-OPS-GR, European Space Operations Centre, Darmstadt, Germany, May 2018.
- [17] T.S. Kelso, Master tle index, NORAD CelesTrak, Accessed January 21, 2019] (Jul. 2019). URL <https://www.celestrak.com/NORAD/elements/master.php>.
- [18] G.D. Krebs, Gunter's space page, [Accessed January 18, 2019] (Aug. 2019). URL <https://space.skyrocket.de/>.
- [19] D. Beale, ESMC Course Material: Fundamentals of Lunar and Systems Engineering for Senior Project Teams, with Application to a Lunar Excavator vol. 9, Auburn University, 2009 9–3, [Accessed January 22, 2019]. URL <http://www.eng.auburn.edu/~dbeale/ESMDCourse/>.
- [20] V. Lempereur, Electrical power systems, Thales Alenia space, [Accessed January 22, 2019] (Nov. 2017). URL http://www.s3l.be/usr/files/di/fi/2/2017_EPS_Lempereur_201811271527.pdf.
- [21] Union of Concerned Scientists, UCS Satellite Database, Union of Concerned Scientists, 2018 Accessed January 18, 2019 <https://www.ucsusa.org/nuclear-weapons/space-weapons/satellite-database#XEBqb89KhTY>.
- [22] D. DeSantis, Satellite Thruster Propulsion- H2O2 Bipropellant Comparison with Existing Alternatives, Department of Space Technologies, Institute of Aviation, The Ohio State University, Ohio, USA, 2014.
- [23] Orbital Propulsion Centre, Lampoldshausen spacecraft propulsion from 1969 to 2031, ArianeGroup, [Accessed January 23, 2019]. URL <http://www.space-propulsion.com/spacecraft-propulsion/heritage/index.html>.
- [24] B.D. Fulcher, N.S. Jones, Highly comparative feature-based time-series classification, IEEE Trans. Knowl. Data Eng. 26 (12) (2014) 3026–3037, <https://doi.org/10.1109/TKDE.2014.2316504>.
- [25] D.R. Williams, Earth fact sheet, national Aeronautics and space administration, Accessed August 24, 2019] (Apr. 2019). URL <https://nssdc.gsfc.nasa.gov/planetary/factsheet/earthfact.html>.
- [26] V.A. Chobotov, Orbital Mechanics, third ed., American Institute of Aeronautics and Astronautics, Reston, Virginia, 2002, <https://doi.org/10.2514/4.862250>.
- [27] J.E. Prussing, Optimal Spacecraft Trajectories, first ed., Oxford University Press, New York, USA, 2018, <https://doi.org/10.1093/oso/9780198811084.001.0001>.
- [28] B. Vincent, Rsgs payload technical overview, robotic servicing of geosynchronous satellites (RSGS) proposers day, [Accessed January 8, 2019] (2016). URL <https://www.darpa.mil/attachments/RSGSProposersDaySlideDeck.PDF>.
- [29] B.D. Fulcher, N.S. Jones, htcsa, A computational framework for automated time-series phenotyping using massive feature extraction, Cell Syst. 5 (5) (2017) 527–531, <https://doi.org/10.1016/j.cels.2017.10.001> e3.